WHITE PAPER

AUGUST 6, 2013

Low-Energy RHIC electron Cooler (LEReC)

Collider-Accelerator Department, BNL

This document describes the present concept and scope of Low Energy RHIC electron Cooling (LEReC) project. The concept is based on using bunched electron beams produced with the SRF accelerator. Electron accelerator will be installed at IR2 in RHIC tunnel.

Table of Contents

1 OVERVIEW

Mapping the QCD phase diagram is one of the fundamental goals of heavy-ion collision experiments. The QCD critical point is a distinct feature of the phase diagram, the existence of which is predicted by various QCD models. The first beam energy scan (BES-I) runs for physics were successfully conducted at RHIC during 2010-11. During BES Phase-I physics runs data sets were collected for Au+Au collisions at 7.7, 11.5, 19.6 and 39 GeV. Driven by physics and BES-I results, future physics program called BES-II is proposed for Au+Au energies below 20 GeV (γ=10.7). However, required event statistics is much higher than previously achieved and relies on significant luminosity improvement in RHIC at energies below γ=10.7 with the help of electron cooling upgrade.

Applying electron cooling directly in RHIC can increase the average integrated luminosity significantly [1-2]. An electron cooling technique requires electron beam co-propagating with the same velocity as the ion beam in a localized portion of circular accelerator called the cooling section. An electron beam up to 5 MeV kinetic energy is required to cover the full energy range of interest, as shown in Table 1. The energy range in Table 1 stops at lowest energy of γ=4.1 (c.m. energy of 7.7 GeV) since RHIC was not able yet to operate at lower energies with conditions suitable for physics program.

Table 1. Beam Energy Scan II (BES-II) energies to be covered by electron cooler.

$\sqrt{s_{NN}}$ GeV (center of mass Au+Au energy)	7.7	11.5	20
γ	4.1	6.2	10.7
Kinetic energy of electron beam, MeV	1.6	2.7	5

The role of electron cooling for the lowest energy points is to counteract intrabeam scattering (IBS): this prevents transverse emittance growth and intensity loss from the RF bucket due to the longitudinal IBS. If IBS were the only limitation, this would allow one to keep the initial peak luminosity close to constant throughout the store essentially without the beam loss (provided that loss of ions due to recombination is counteracted, and acceptance of the RF bucket is sufficient). In addition, the phase-space density of the hadron beams can be further increased by providing stronger electron cooling. Unfortunately, the defining limitation for low energies in RHIC is expected to be the space charge [3], which prohibits strong cooling at lowest energies of interest. Experimental studies of the space-charge effects and beam lifetime in RHIC were conducted and reported in Refs. [4-5]. As the energy is increased, the space-charge effect on the hadron beam becomes smaller which permits cooling of the transverse or longitudinal emittances of the hadron beams as well, allowing in turn to reduce the β^*. During RHIC operation at γ=4.1 and measured fast time component of the beam lifetime decay was shorter than expected from the IBS and was attributed to other effects [4-7]. At even lower energies ($\gamma < 4$) dynamic aperture is expected to be very small [8] which would require operation with very small transverse emittance resulting in a very strong IBS, making cooling a requirement for successful operation.

Since space-charge driven beam lifetime prohibits strong cooling of beam emittance or bunch length at lowest energies, an approach of operation with longer bunch length (low-frequency RF)

was suggested [9]. Further advantages of the new low-frequency RF system include a possibility to provide a wide range of energies available for physics as described in Ref. [10].

Overall possible projection of luminosity improvement as a function of energy is shown in Fig. 1 (for details see Ref. [11]). As indicated by the blue dash line, expected luminosity improvement could be rather modest at lowest energy points if one employs existing 28 MHz RF system. The curves stop at lowest energy of γ=4.1 (Au-Au c.m. energy of 7.7 GeV) since RHIC was not able yet to operate at lower energies with conditions suitable for physics program.

Since operation with longer bunches (requires RHIC upgrade with new low-frequency RF) allows us to apply significant transverse cooling which should improve beam lifetime at lowest energies, it offers better path forward towards luminosity improvement, as indicated by the top magenta line in Fig. 1. Note that projection of luminosity improvement using low-frequency RF system and long ion bunches shown by the magenta line corresponds to an ideal improvement (with beam lifetime driven by IBS only which is assumed to be counteracted successfully by electron cooling). The purpose of such a projection is just to indicate a potential for maximum possible luminosity improvement with longer bunches. Such projection does not include beam lifetime limitations observed at lowest energies for large values of the space-charge tune spread and additional limitations caused by the beam-beam effects. In reality, achievable luminosity will be somewhat smaller than indicated by the magenta line (blue dash line for the 28 MHz RF) because of the uncertainty how electron cooling can improve the beam lifetime not associated with IBS and due to a required experimental optimization between various processes, including 3-D electron cooling (this will be the first electron cooling in a collider), ion beam loss on recombination and beam lifetime.

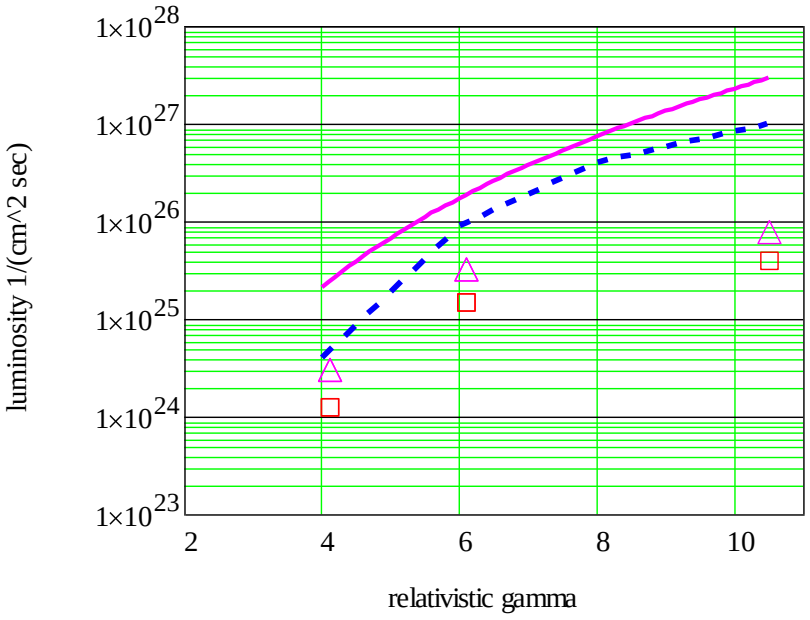

Figure 1. Projection of possible average per store luminosity in RHIC with electron cooling upgrade (for 111 bunches). Red squares: measured average per store luminosity in BES-I; magenta triangles: measured maximum luminosity during BES-I; blue dash line: expected luminosity improvement with cooling and present 28 MHz RF system. Magenta top solid line: with cooling and long ion bunches (with proposed new low-frequency RF system in RHIC).

2 LOCATION AND LAYOUT

An SRF gun based injector for LEReC will be located near IR2 and will use the same cryogenic system as the Coherent Electron Cooling Proof-of-Principle (CEC PoP) experiment. Two electron cooling sections (one for the Yellow and one for the Blue RHIC rings) will be located in Warm Sector 2.

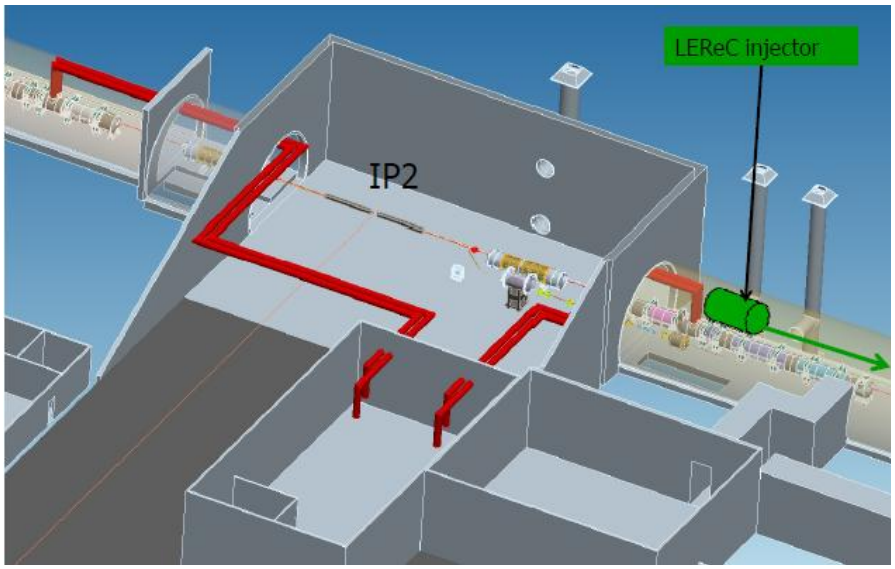

Figure 2. Location of SRF accelerator for electron cooler in IR2.

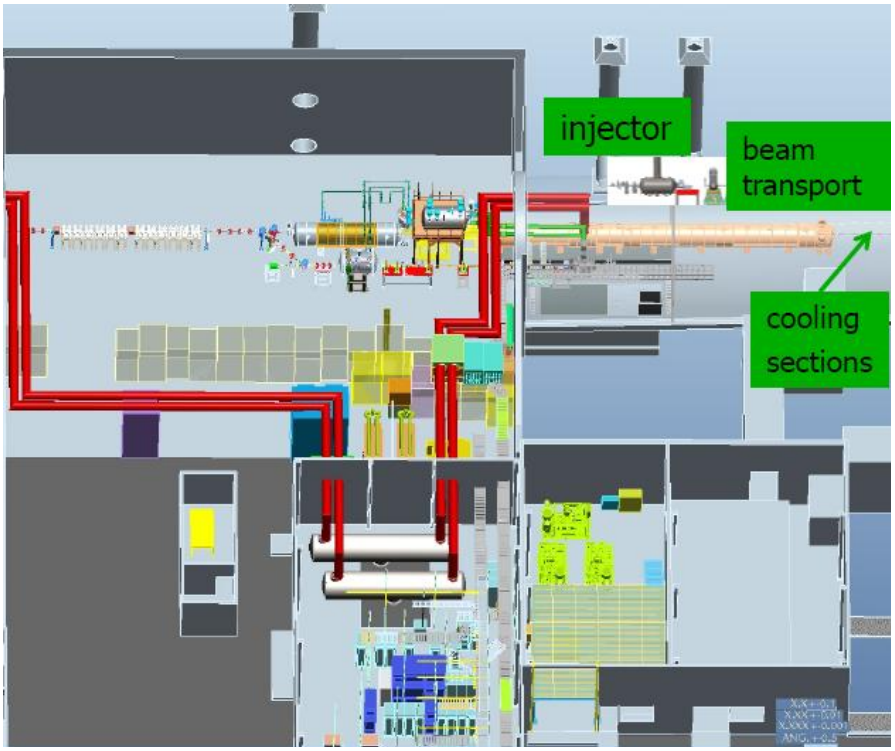

Figure 3: Schematic location of electron accelerator at IR2, with electron cooling sections located in warm sector 2.

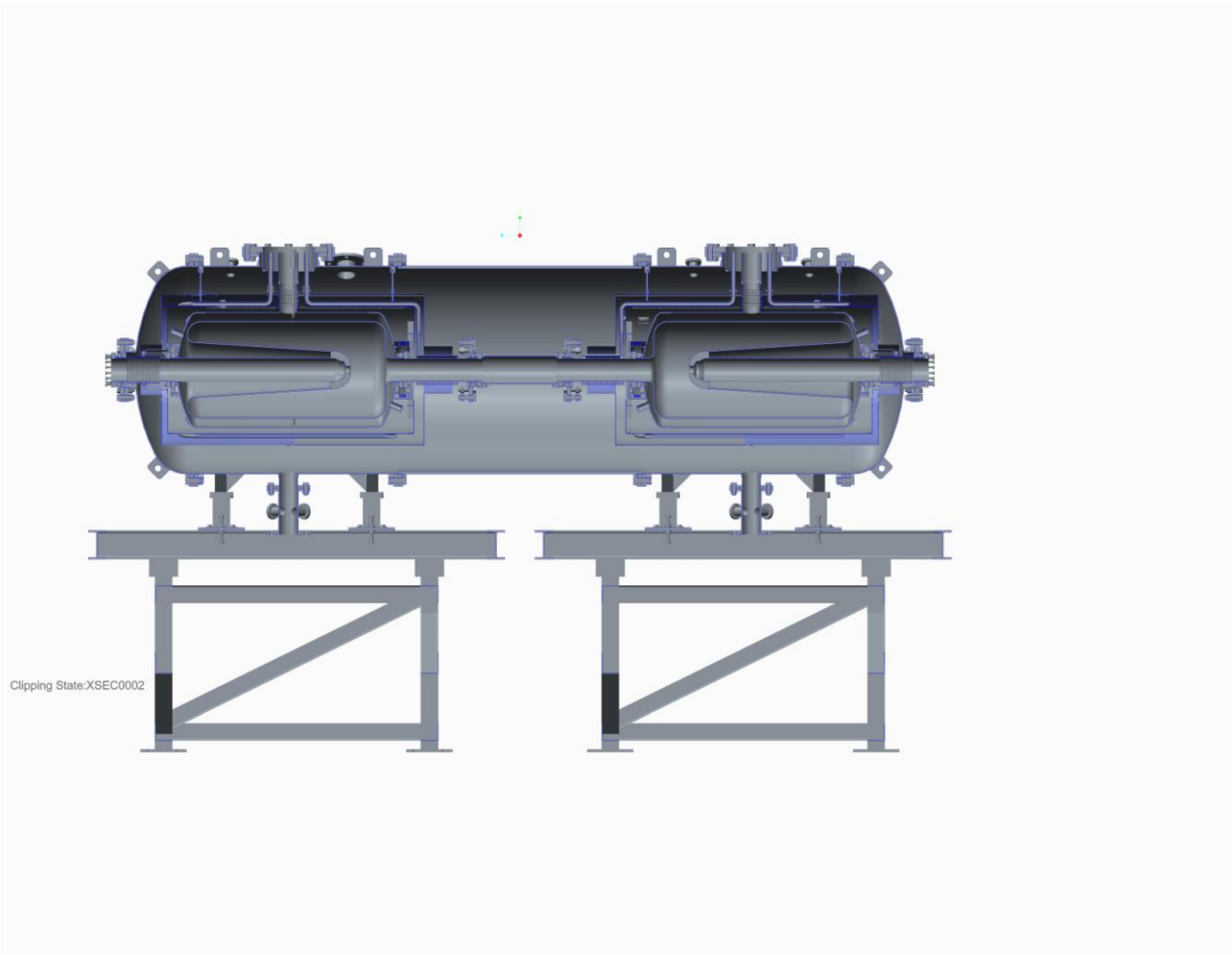

Figure 4: Schematic of the SRF accelerator (photoemission gun and booster cavity in a single cryostat). Shown are scaled versions of the 112 MHz SRF gun cavity used for CeC project, not the final design.

An electron beam line will be located in the 02:00 IP area mostly between the Q2 magnet in the RHIC 02:00 sector and the Q4 magnet in the RHIC 02:00 sector.

Support equipment will be located in 1002A and 1002B; but, space is limited in those buildings and an AC upgrade may be needed in the 1002A control room to deal with the added equipment.

A new laser building has been already ordered for the CeC project and will be used for the LEReC project as well (1002C or 1002E).

Building 1002D, presently used for the AnDY experiment (previously used for BRAHMS), will be used for power supplies and controls equipment that can not fit in 1002A and B.

3 THE SCOPE OF ELECTRON COOLER

The Electron Cooler will consist of:

1. A 100 MHz SRF photoemission gun with maximum energy of 2.5 MeV.
2. A 100 MHz SRF booster cavity providing maximum energy gain of 2.5 MeV, housed in the same cryostat with the gun.
3. A superconducting solenoid (about 1 kGauss) inside the cryostat between the gun and the cavity.
4. A 500 MHz (5^{th} harmonic of the SRF frequency) copper cavity for energy spread correction.
5. Electron beam transport form IR2 section to the cooling section in warm sector 2.
6. Cooling section in Blue RHIC ring – 12 m long. Short (10 cm) correction solenoids located every 2 m. Free space between the solenoids is covered by several layers of the mu metal to shield magnetic field to a required level or Helmholts coils for active correction.
7. U-turn magnet between cooling section in Blue and Yellow Rings.
8. Cooling section in Yellow Ring.
9. Dump for the electron beam.
10. Beam transport magnets and diagnostics.

4 ELECTRON COOLER PARAMETERS

Luminosity improvement needed requires electron beam with kinetic energy up to 5 MeV. Electron cooler is presently being optimized for operation in the range of γ=4-10.7 (Au-Au c.m. energies 7.7-20 GeV). Operation with energies below 1.6 MeV ($< \gamma$=4) is also being considered.

4.1 Electron beam parameters

An upgrade of RHIC RF with new 4.5 MHz system, which would allow use of longer bunches, is presently being evaluated. Electron beam parameters presented below are given based on cooling of ions beams with such new 4.5 MHz RF. To control longitudinal IBS rates the mode of operation with large longitudinal emittances was identified which in turn required significant RF voltage of 80 kV [12].

Depending on beam energy and longitudinal emittance, the ion beam will have rms longitudinal momentum spread in the range of σ_p=4 - 5×10^{-4}. This sets a limit on the rms momentum spread of electron beam of $< 5\times10^{-4}$.

The requirement on transverse angles of electron beam in the cooling section is given by the angular spread of the ion beam in the cooling section. For example, for rms normalized emittance of 2.5 mm-mrad at γ=4.1, and 30 m beta function in the cooling section, the ion beam rms angular spread in the lab frame is 0.144 mrad. Electron cooling will be provided with a train of electron bunches place on single ion bunch (see requirement on total electron charge to be spread over ion bunch. Some parameters of the cooler are summarized in Table 2.

Table 2: Parameters for electron beam needed for cooling.

	γ=4.1	γ=10.7	γ=10.7
RHIC RF frequency, MHz	4.55	4.67	28
Electron kinetic energy, MeV	1.6	5	5
Total charge Q, nC	4.0 (spread over 9 bunches)	7 (spread over 5 bunches)	4 (spread over 2 bunches)
dp/p, rms	5e-4	5e-4	5e-4
Transverse angular spread, μrad (contribution from all sources, "effective spread" – angular budget)	<150	<90	<90
Emittance, n, rms,	2.5	2.5	2.5
Transverse rms size, mm	4.3	2.6	2.6
Full bunch length, ns	0.5-1	0.5-1	0.5-1
Cooling length, m	12	12	12
Nominal electron current, mA	18	33	36
Beam power, kW	29	165	180

New 4.5 MHz RHIC RF system will be tunable in the full energy range of interest which will allow fine steps in future physics energy scans. For completeness, Table 2 also shows parameters of electron beam for cooling of ion bunches using present 28 MHz RHIC RF. Without changing RF harmonic h=360, such system can be used for cooling at energies of γ=7.8-10.7, where we are not limited by the space charge or acceptance of the RF bucket.

Table 3 lists parameters of undulator which allows to suppress loss of heavy ion on recombination with electron beam. However, it appears that without suppression of recombination resulting loss in integrated luminosity is negligible. Thus, for the baseline approach we do not require undulators and will not have recombination suppression (this could be a possible future upgrade).

Table 3: Undulator parameters for recombination suppression.

Undulator magnetic field, G	3
Undulator period, cm	8

4.2 Cooling approach

In low-energy electron coolers a magnetic field is required to provide transport of the electron beam. For energies of 1 MeV and higher needed for our project, continuous magnetic field transport is no longer required. However, in the cooling section, the interaction of the ion and electron beams results in ion beam loss due to recombination. Employment of strong magnetic field in the cooling section allows one to incorporate a large transverse temperature of the electron beam for

recombination suppression. On the other hand, suppression of ion recombination can be achieved with rather weak undulator field in the cooling section still allowing non-magnetized beam transport. Since non-magnetized cooling significantly simplifies electron beam transport and reduces the cost of the cooler, it was chosen as our baseline approach.

Due to a relatively small required current, an approach with zero magnetic field on the cathode and thus no magnetic field in the cooling section is also feasible. In this case, only short corrector solenoids every 2 m will be needed to provide needed focusing in the cooling section. Such an approach would correspond to a pure case of "non-magnetized" cooling.

The use of undulators for recombination suppression in the cooling section is compatible with approach chosen. However, the use of undulators would require significant engineering modification of the cooling section while the expected benefit in luminosity with recombination suppression seems rather modest. Presently, recombination suppression with undulators is not included in the baseline.

4.3 Ion beams

Ion beam in two RHIC rings presently operate at slightly different energy. For cooling process energy of electron beam has to coincide with the one of ions better than rms energy spread of the ion beam. Since, depending on RF voltage and longitudinal beam emittance, rms ion energy spread could be as low as 4e-4, energy of electrons needs to agree with energy of ions to better than 4e-4.

Since cooling in both ions rings will be provided using the same electron beam, energy of ions in the second RHIC ring will need to be adjusted to match energy of electron beam (or energy of electron beam will need to be corrected accordingly after the first cooling section).

Up to +/-25mA fluctuations of current could be expected in the main RHIC dipoles. For energies of interest this corresponds to up to dp/p=1e-5 energy ripple which is acceptable.

4.4 Ion beam lattice

RHIC lattice is designed to have an appropriate ion beta-function in the cooling section. The beta-functions close to 30 meters are presently being considered in the cooling section. Such beta-function will be kept close to constant during the length of the cooling section. Smaller beta-functions result in larger angular spread of ion beam and thus make requirement on angular spread of electron beam less strict. Several versions of RHIC optics for LEReC were already developed. One of the solutions is shown in Figs. 5-8, as an example.

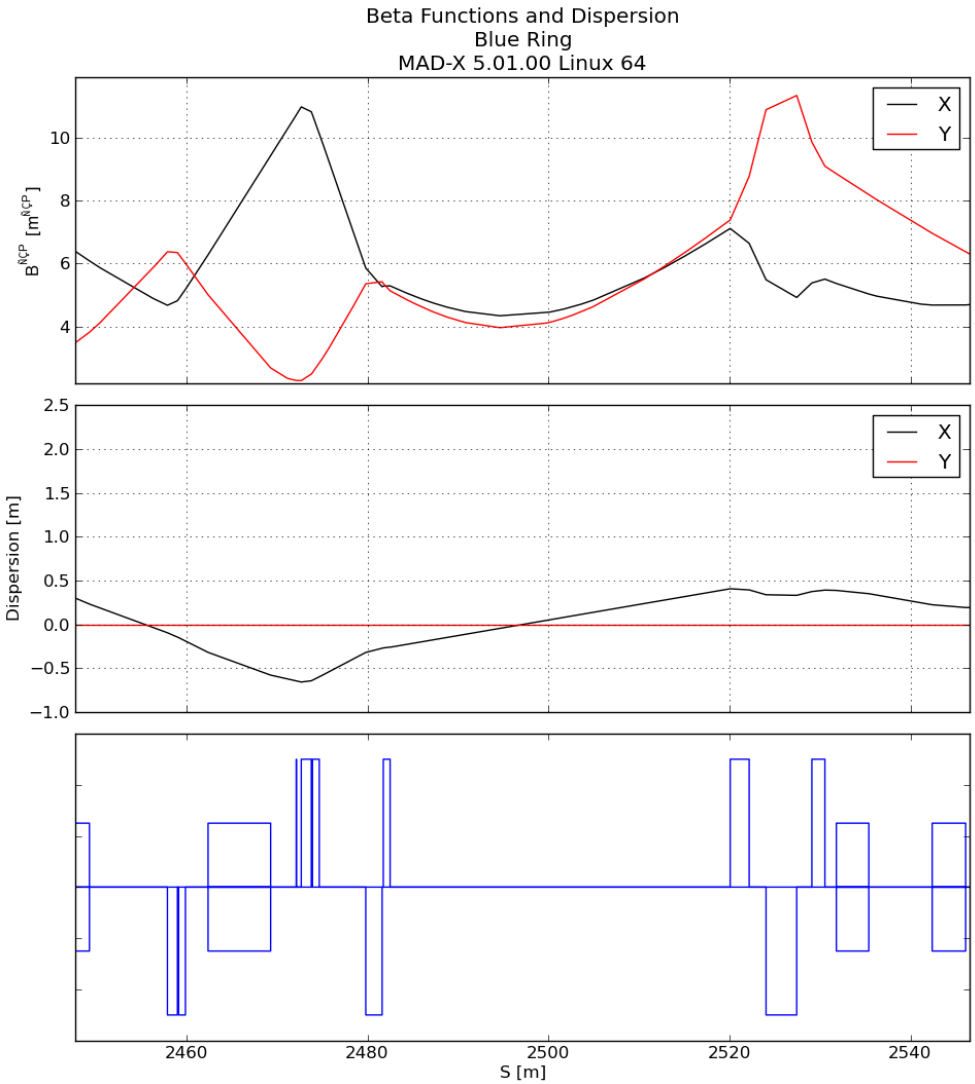

Figure 5. RHIC optics for cooling section in blue ring.

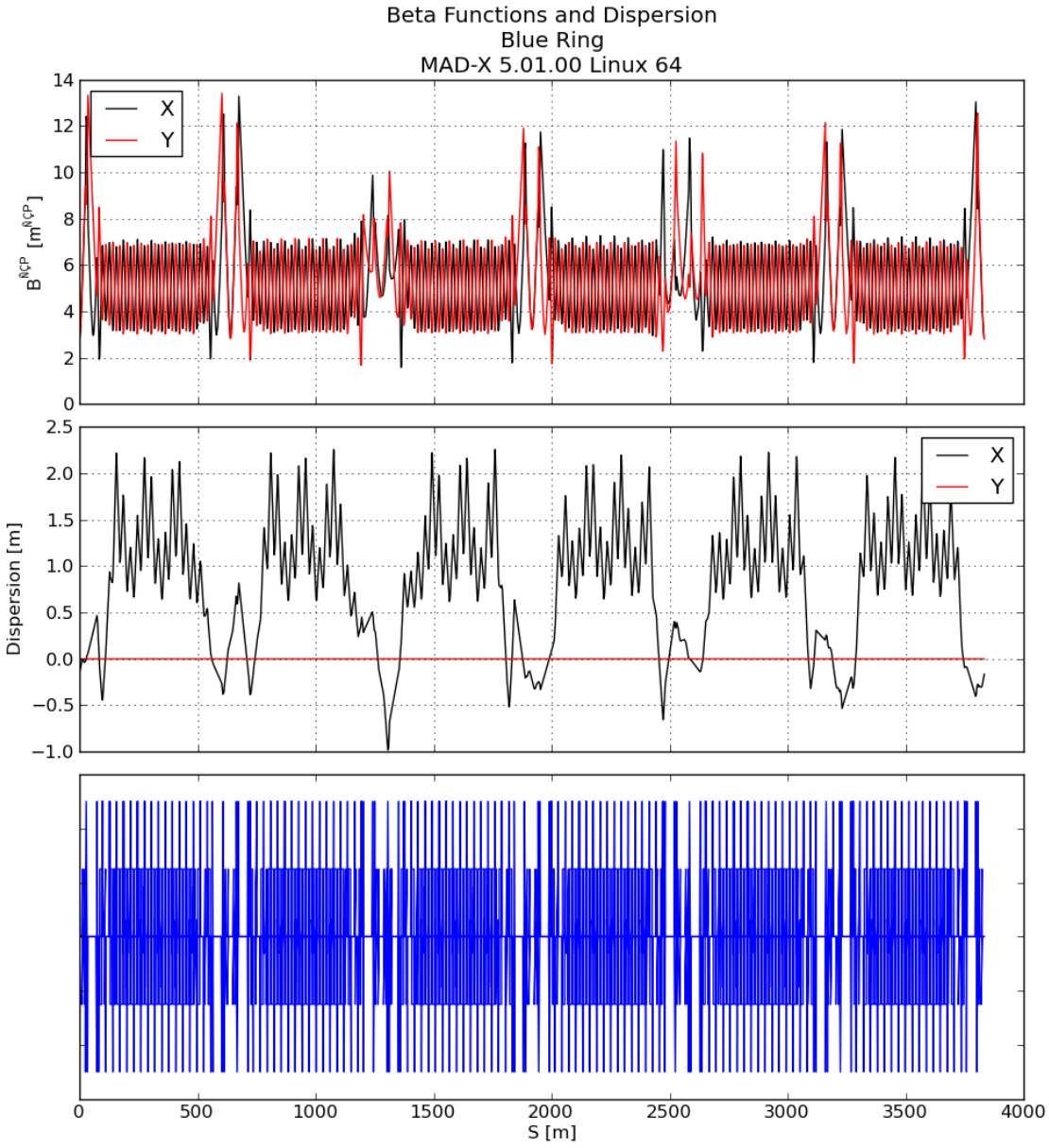

Figure 6. Full blue Ring RHIC LEReC optics.

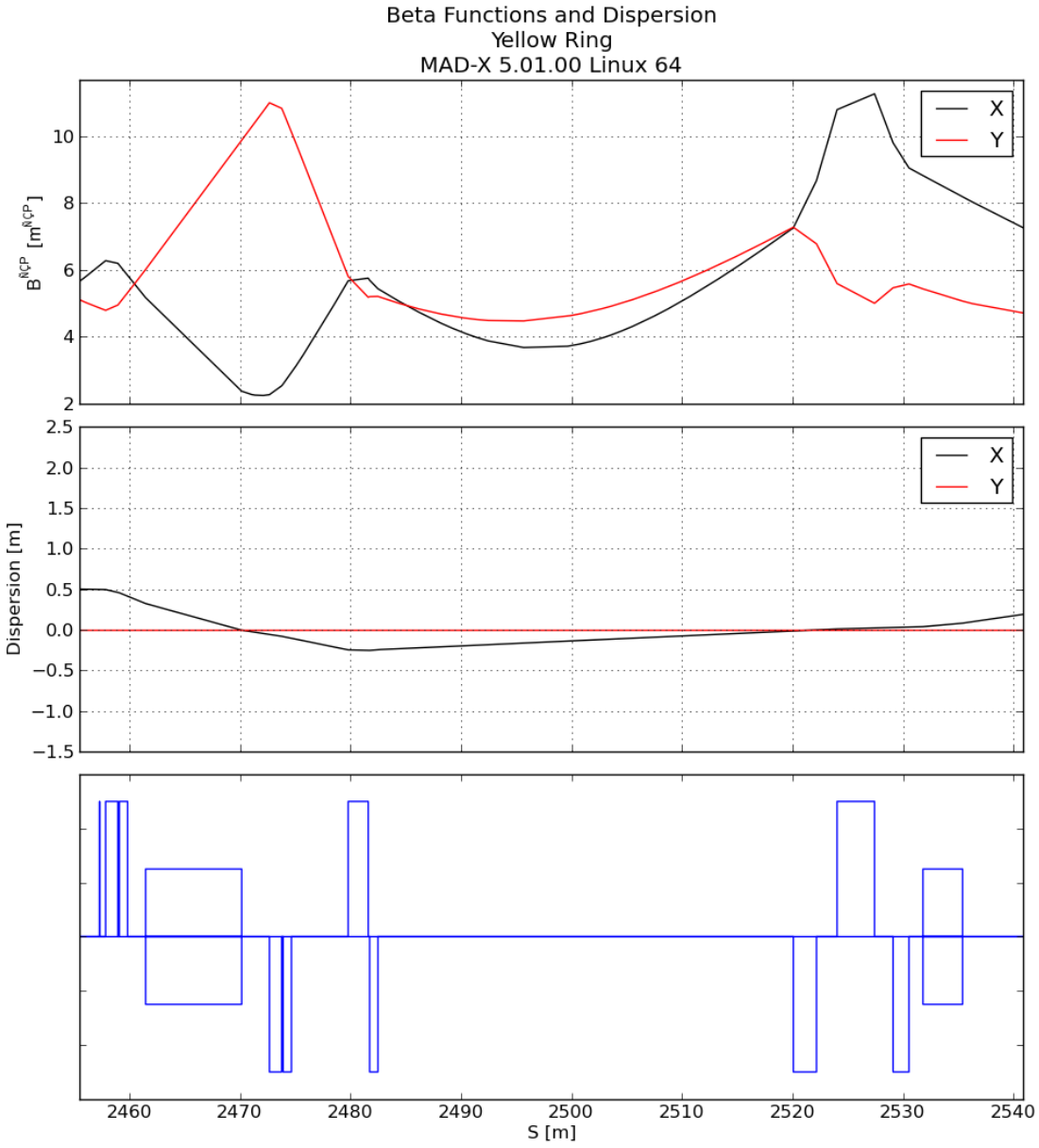

Figure 7. RHIC optics for cooling section in yellow ring.

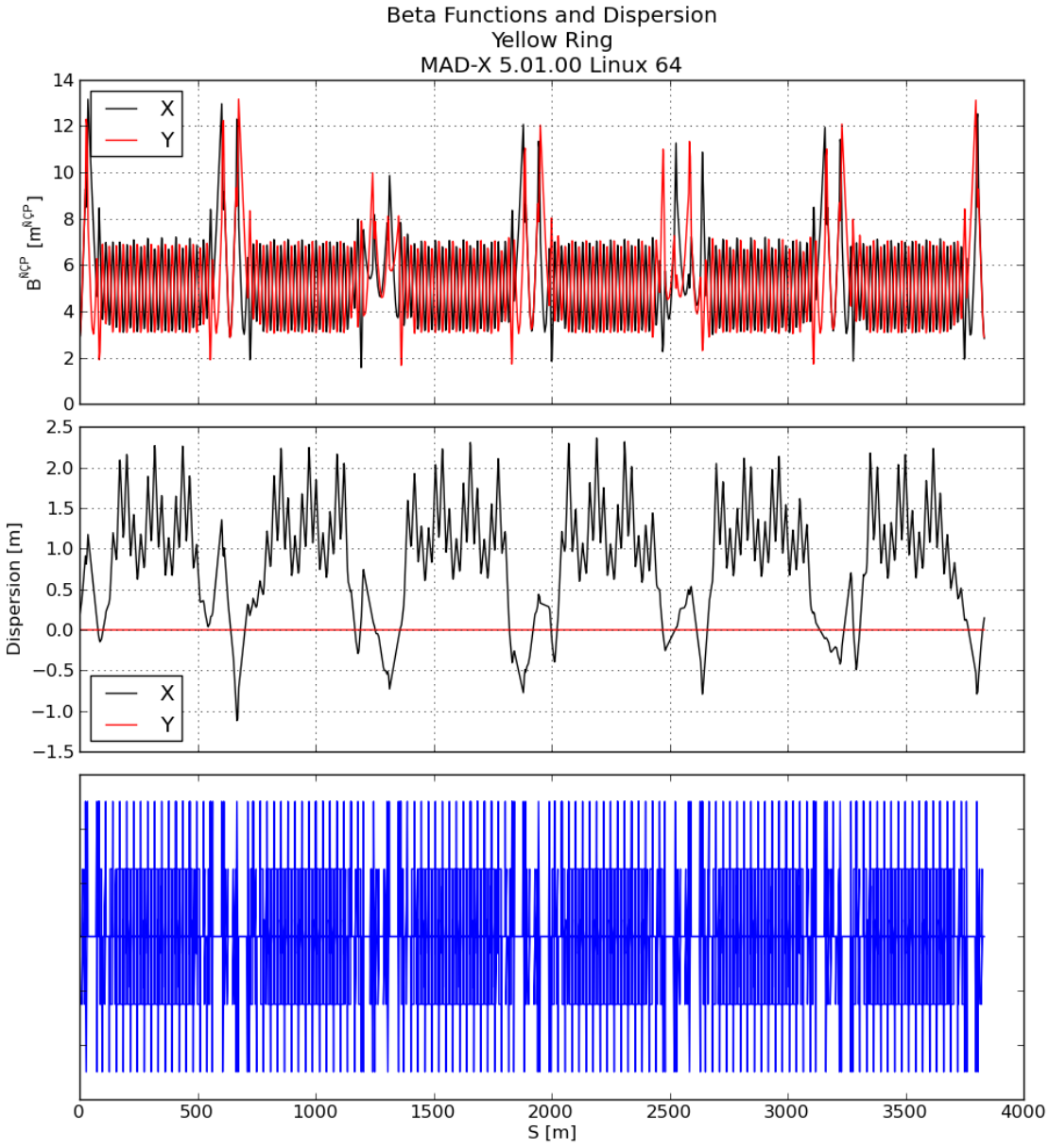

Figure 8. Full yellow Ring RHIC LEReC optics.

5 ELECTRON ACCELERATOR

The electron accelerator (linac) will consist of a two-cavity superconducting RF (SRF) cryomodule producing beam with energy up to 5 MeV and a 500 MHz normal conducting cavity for energy spread correction. The cryomodule will house a photoemission SRF gun and an SRF booster cavity, both operating at 100 MHz. There will be a superconducting solenoid between the two cavities. Parameters of the linac are listed in Table 4.

Electron beam will be generated by illuminating an CsK_2Sb photocathode with green (532 nm) light from a laser. The photocathode is inserted into a 100 MHz quarter-wave SRF cavity thus forming an SRF photoemission electron gun. The photocathode is located in a high electric field. Immediate acceleration of the electrons to a high energy reduces emittance degradation caused by a strong non-linear space-charge force. The low RF frequency of the gun reduces effect of RF curvature on the beam. The gun will produce bunch trains with relatively long electron bunches, about 750 ps, at 100 MHz bunch repetition frequency. The bunch train repetition rate will be the same as repetition rate of ion bunches in RHIC. The optical system will allow creating dedicated bunch patterns for different RHIC energies and ion bunch lengths with several bunches at 100 MHz frequency followed by a long gap corresponding to the frequency of ion bunches.

While the required beam current has yet to be demonstrated from an SRF gun, even higher beam currents were already achieved from photocathodes in an RF gun [13] and a DC gun [14]. Three types of high QE photocathodes are used nowadays in SRF guns: GaAs(Cs), Cs_2Te, and CsK_2Sb [15, 16]. On the one hand, cesium potassium antimonide cathodes are more robust than gallium arsenide ones as they have very long lifetime [14] and can be transported without much degradation of their performance [17]. On the other hand, they have higher QE than cesium telluride cathodes and can be used with green lasers. CsK_2Sb is the most preferred option at present [18].

The SRF gun design will be similar to the 112 MHz SRF gun developed for the CeC PoP experiment at BNL [19], shown in Figure 9, with the following major differences: 1) The gun cavity shape will be optimized to improve surface fields and reduce wall losses; 2) The gun will be equipped with two high-power fundamental RF power couplers; 3) There will be a frequency tuner of an improved design. The cathode insertion mechanism and the photocathode stalk will be scaled copies of the 112 MHz gun designs [20].

The cavity shape optimization goals are to keep the peak surface electric and magnetic fields below 40 MV/m and 80 mT correspondingly, and to improve the cavity RF performance. The surface fields cited above are accepted in the SRF community as “rule of thumb” design goals for CW operations. As the beam pipe aperture in LEReC injector is reduced from 10 cm to 5 cm as compared to CeC PoP, it makes it easier to achieve the desired peak surface fields in the cavities. Preliminary optimization of the cavity shape, performed in collaboration with ANL, shows that achieving the goals is possible. ANL has proven record of designing and building high performing SRF cavities of complex shapes that typically exceed the LEReC requirements for maximum surface fields [21, 22]. Also, they have experience in incorporating superconducting solenoids in SRF cryomodules. We plan to design, fabricate, process and test SRF cavities in close collaboration with ANL.

Table 4: Parameters of the LEReC electron linac.

Beam			
Lorentz factor	4.1	10.7	10.7
RHIC RF frequency, MHz	4.55	4.67	28.03
Electron beam kinetic energy, MeV	1.58	4.96	4.96
Total charge, nC	4.0 (9 bunches)	7 (5 bunches)	4 (2 bunches)
$\Delta p/p$, rms	5e-4	5e-4	5e-4
Normalized rms emittance, mm.mrad	2.5	2.5	2.5
Transverse rms size, mm	4.3	2.6	2.6
Full bunch length, ns	0.5-1	0.5-1	0.5-1
Electron beam current, mA	18.2	32.7	35.8
Beam power, kW	28.8	162	178
SRF gun and booster			
SRF frequency, MHz	100.00	99.97	99.97
Gun voltage, MV	1.65	2.58	2.58
Epk, MV/m	25.4	39.7	39.7
Bpk, mT	48.5	75.8	75.8
R/Q, Ohm	162.2	162.2	162.2
Geometry factor, Ohm	47.6	47.6	47.6
Cavity *Q* factor	3.4e9	3.4e9	3.4e9
Gun cavity power dissipation at 4.5 K, W	5	12	12
External *Q* factor	4e5	4e5	4e5
Gun RF power, kW	31	85	93
Frequency tuning range, kHz	78	78	78
Booster voltage, MV	0	2.58	2.58
Booster RF power, kW	0	85	93
Energy spread compensator			
RF frequency, MHz	500.13	499.82	499.82
Cavity voltage, MV	0.063	0.198	0.198
Shunt impedance, MOhm	5.53	5.53	5.53
Cavity wall dissipation, kW	0.73	7.1	7.1
External *Q* factor (cavity is matched w/o beam)	31,000	31,000	31,000
RF power with beam, kW	0.31	2.1	1.8
Superconducting solenoid			
Magnetic field, T	0.1	0.1	0.1
Laser and cathode			
Wavelength, nm	532	532	532
Quantum efficiency, %	5	5	5
Average optical power on cathode, W	0.85	1.52	1.67
Laser pulse energy, nJ	20.7	65.3	93.2
Peak optical power on cathode, W	41.4	130.5	186.4
Rms time jitter, ps	100	100	100
Rms bunch charge jitter, %	7	7	7

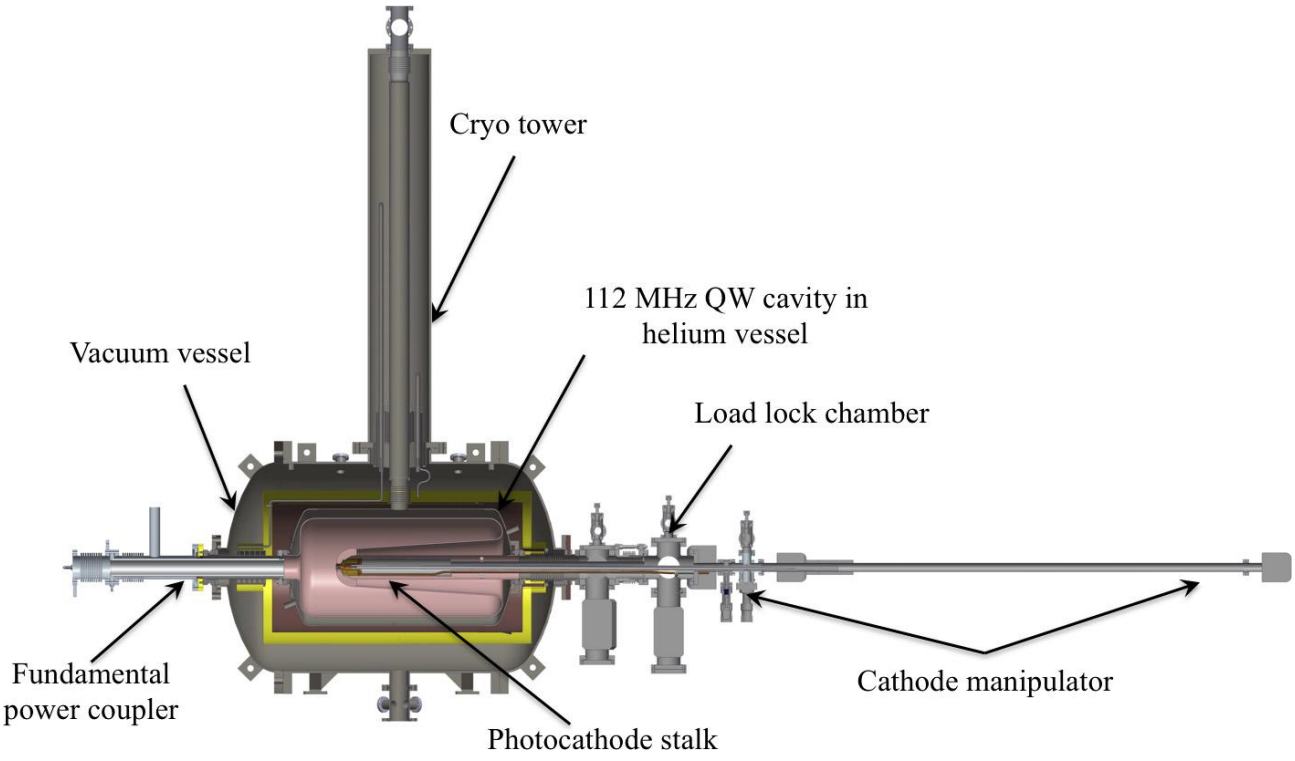

Figure 9: The 112 MHz CeC PoP SRF gun cryomodule.

The booster cavity will be of a similar design as the gun, but with a simplified center conductor as there will be no need to accommodate the photocathode stalk. Both cavities will be designed to provide energy gain up to 2.6 MeV per cavity. At lower energies the booster cavity might be turned off and detuned to become "transparent" to the beam. Figure 10 shows one of optimized geometries proposed for the SRF cavities. Both SRF gun and booster cavity will be housed in a single cryostat with a superconducting solenoid occupying space between them.

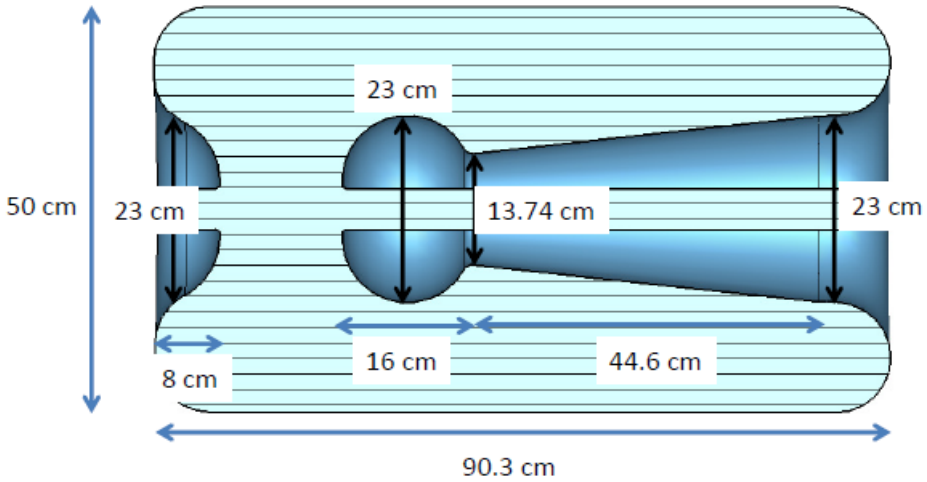

Figure 10: One of the optimized geometries proposed for the 100 MHz SRF booster cavity proposed by ANL [23]. This geometry has lower surface fields and higher $G \cdot R/Q$ parameter than the original 112 MHz SRF gun cavity.

The RF power, up to 93 kW per cavity, will be delivered via two symmetrically located fundamental power couplers. The couplers will be of coaxial antenna type. Computer simulations show that the SNS-type coaxial RF window has very good RF properties at 100 MHz. At SNS, these windows operate at average RF power exceeding 100 kW. At BNL, we use similar windows in FPCs of the ERL SRF gun and five-cell cavity.

Sinusoidal shape of the SRF voltage introduces a quadratic beam energy spread due to on-crest acceleration. To bring the energy spread within required $5 \cdot 10^{-4}$, we plan to use a 5th harmonic normal conducting copper cavity. Correction of the energy spread will require an acceleration voltage up to 200 kV.

6 ELECTRON BEAM TRANSPORT

Schematic layout of electron cooler near 02:00 IP area is shown in Fig. 11.

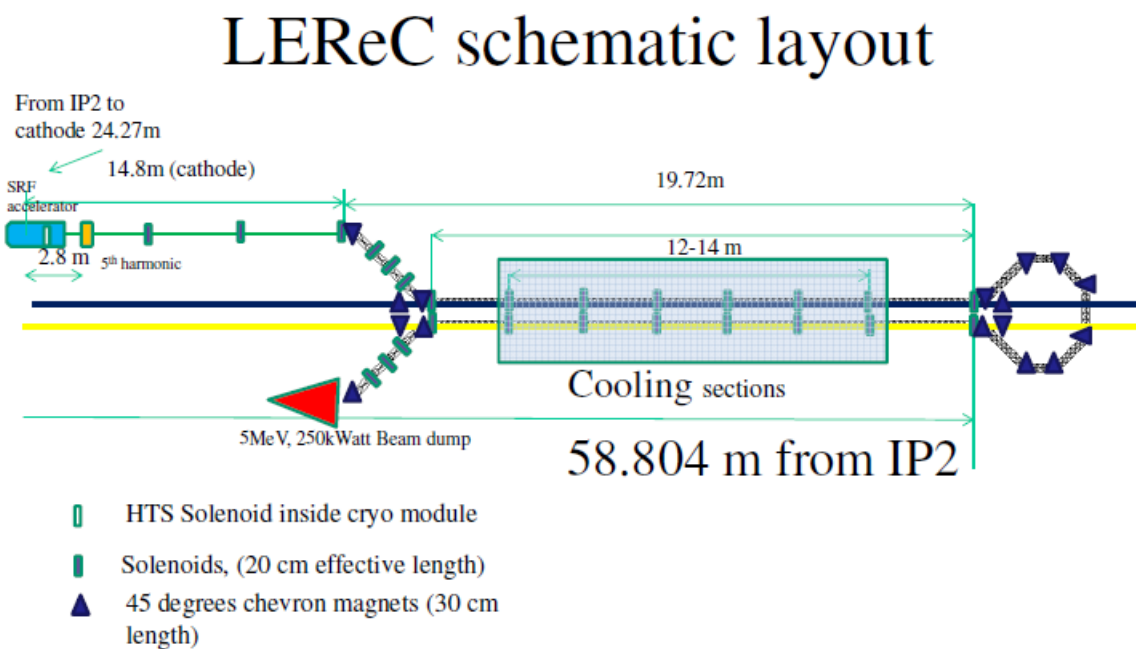

Figure 11. Schematic layout of electron cooler in RHIC Warm Sector 2.

Detailed simulations of electron beam transport from the SRF accelerator to the cooling sections, U-turn between Blue and Yellow RHIC rings and transport to the beam dump are in progress. Preliminary lattice of electron beam transport is shown in Figs. 12-14.

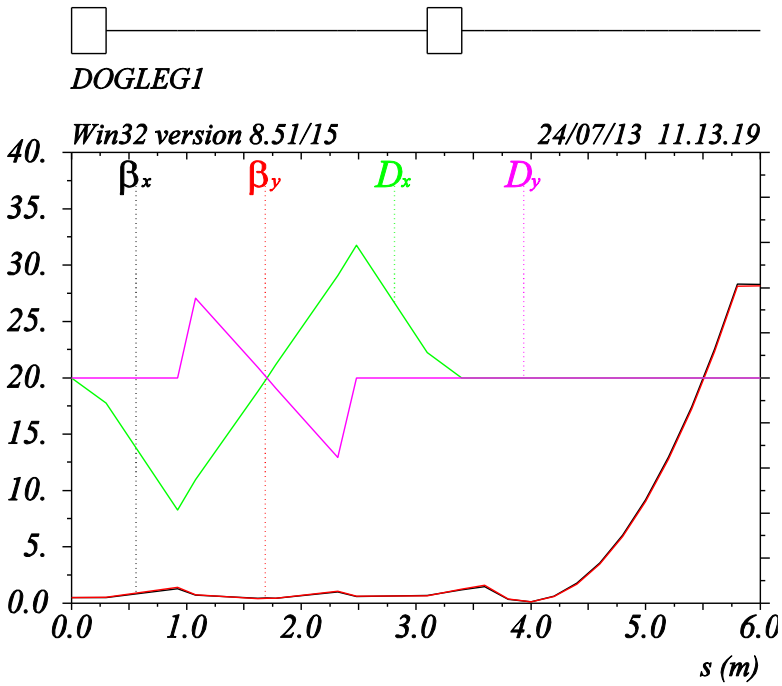

Figure 12. Dog-leg merger of electron beam to the ion beam in RHIC.

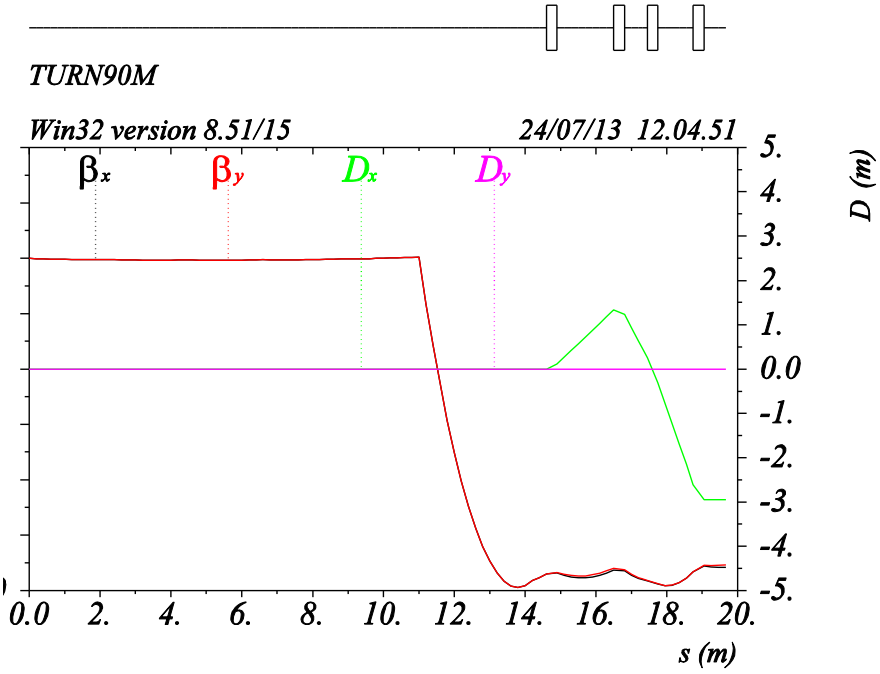

Figure 13. Cooling section and half of the U-turn electron beam line.

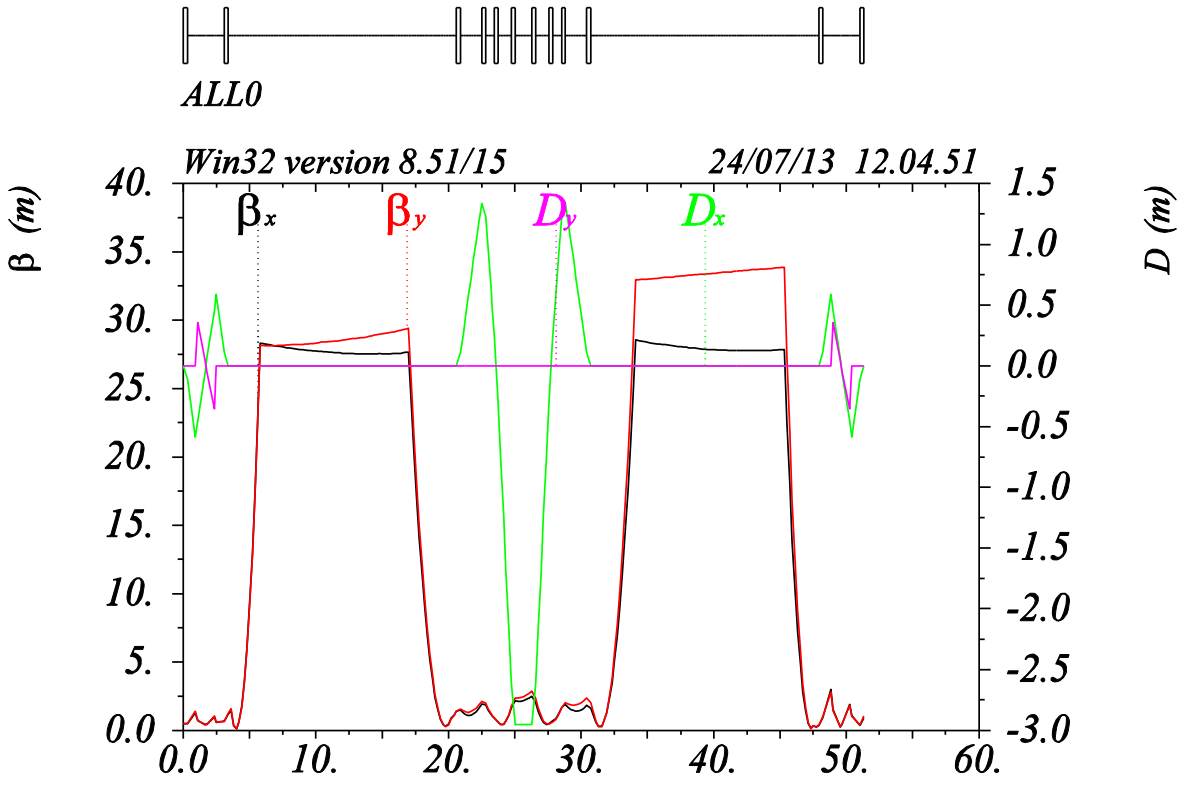

Figure 14. Injection, cooling section in Blue ring, U-turn and cooling section in Yellow ring.

Electron cooling will be provided with a train of electron bunches placed on a single ion bunch (see requirement on total electron charge to be spread over ion bunch in Table 2). For very long ion bunches at lowest energies with new 4.5 MHz RF we can place up to 9 electrons bunches on a single ion bunch (see Fig. 15a). For highest energy of γ=10.7 with new RF system we can place 5 electron bunches on a single ion bunch (Fig. 15b). Also, for highest energies we can use present 28 MHz RHIC RF which allows us to use 2 or 3 electron bunches synchronized with each ion bunch, as shown in Fig. 16. The laser will produce the bunch pattern needed.

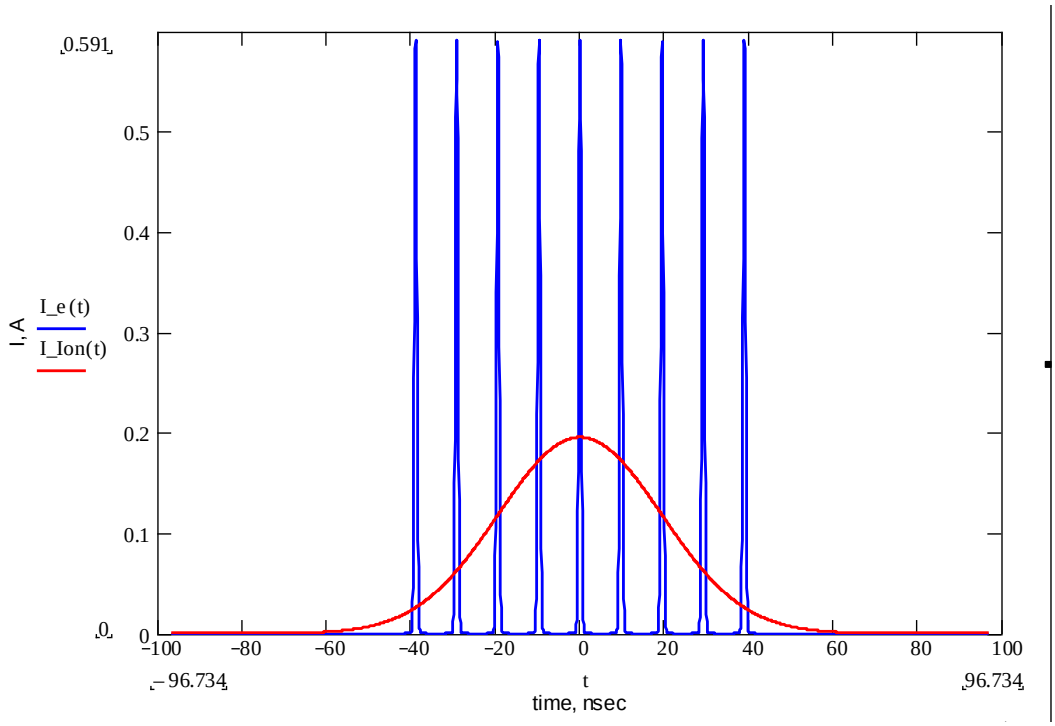

Figure 15a. Nine electron bunches (blue) placed on a single ion bunch (red). Example for long bunches with 4.55 MHz RHIC RF at γ=4.

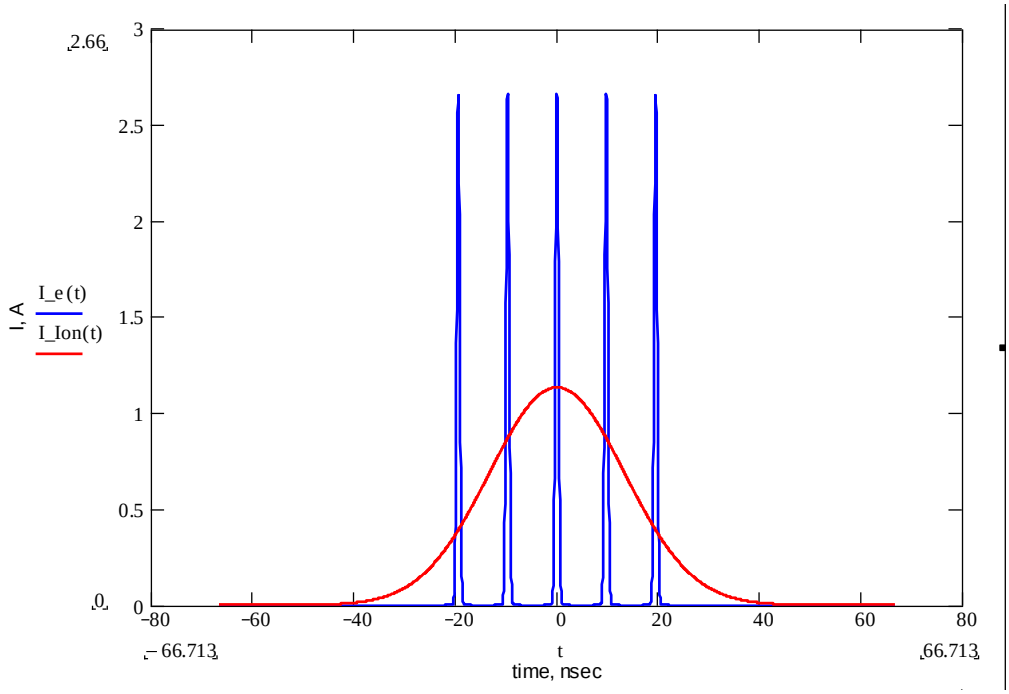

Figure 15b. Five electron bunches (blue) placed on a single ion bunch (red). Example for long bunches with 4.7 MHz RHIC RF and γ=10.

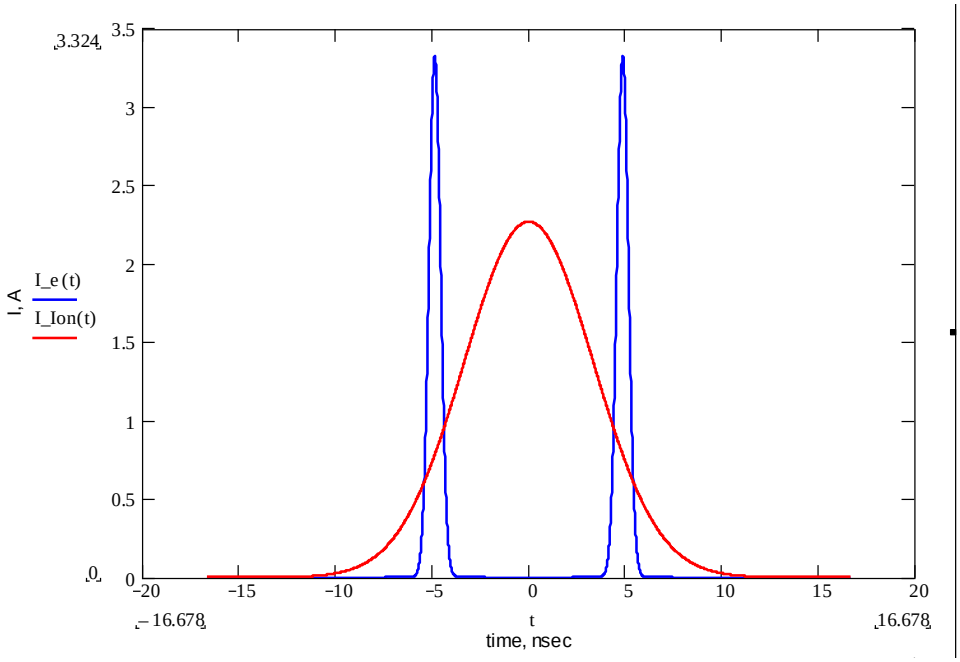

Figure 16. Two electron bunches (blue) placed on single ion bunch (red). Example for short ion bunches using present 28 MHz RHIC RF (at γ=10).

Some results of electron beam dynamics simulations (work in progress) are shown in Figs. 17-19.

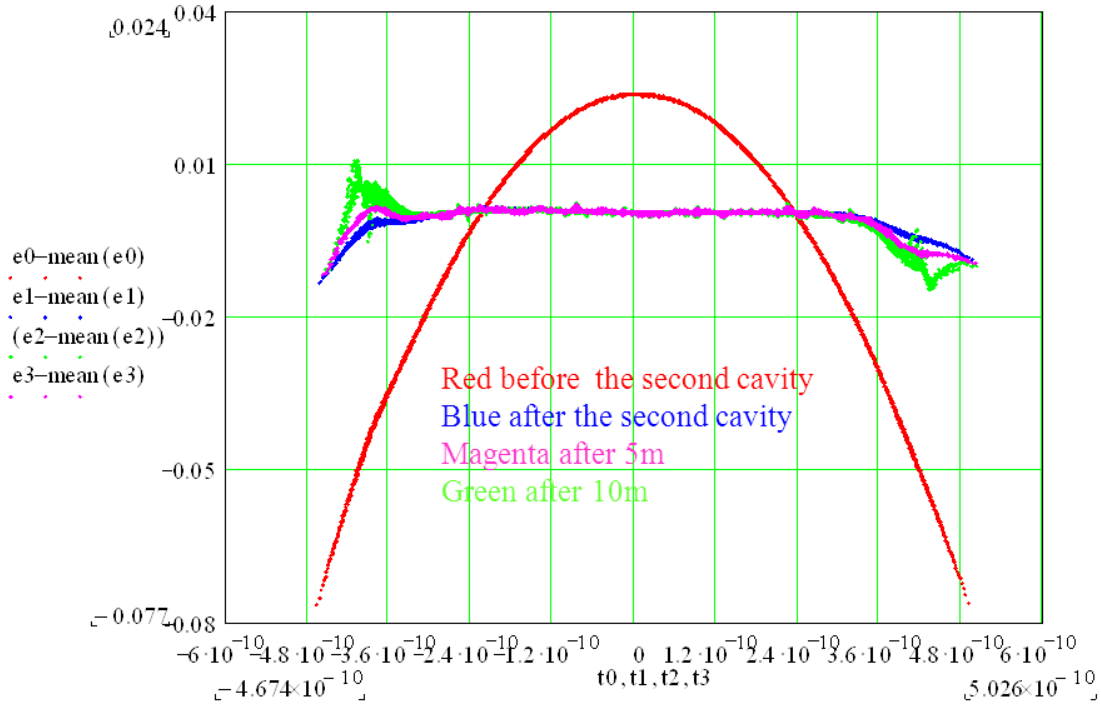

Figure 17. Correction of electron beam energy spread introduced by RF curvature using 5th harmonic correction cavity.

Figure 18. Simulation of tansverse rms angular spread of electron beam along the cooling section (different color represents different portion of the beam: green 100%, red 90%, blue 80%). Upper plot: solenoids every 2m; lower plot: solenoids every 1m.

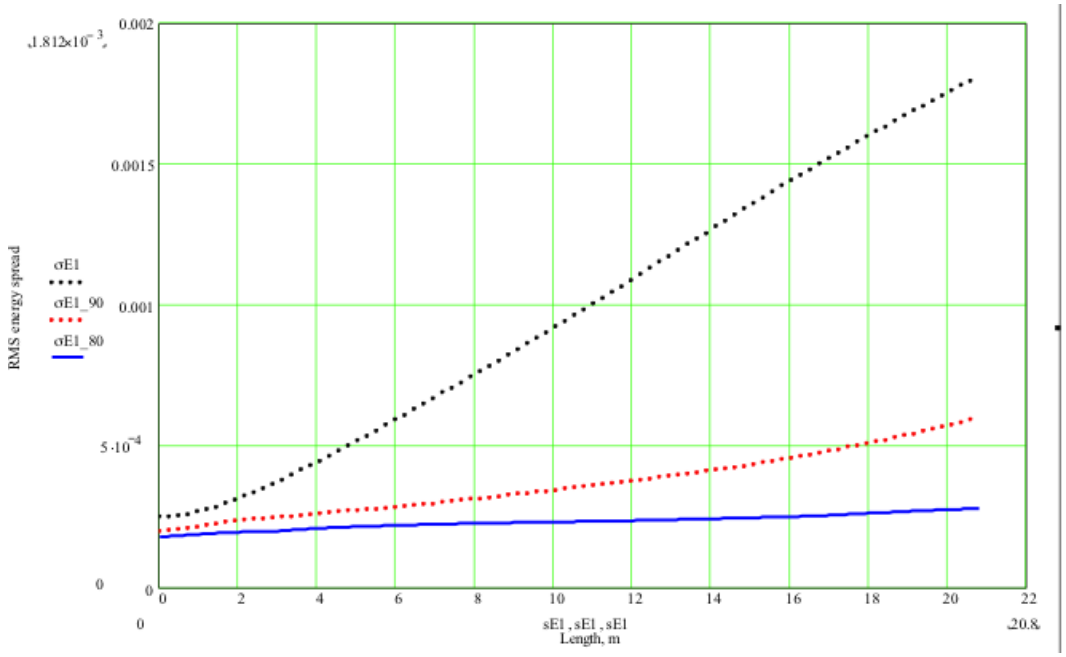

Figure 19. Simulation of rms energy spread within electron beam along the cooling section (different color represents different portion of the beam: black 100%, red 90%, blue 80%).

7 COOLING SECTION

The cooling section is the region where the electron beam overlaps and co-propagates with the ion beam to produce cooling. The electron beam first cools ions in Blue RHIC ring then it is turned around (U-turn) and cools ions in Yellow RHIC ring, after which electron beam goes to the dump. The electron beam must maintain its good quality all the way through the second cooling section in Yellow ring.

The Blue and Yellow ring cooling sections are about 14 meters each (exact length to be determined after new location for some diagnostic devices is fixed). No recombination suppression is planned (as possible future upgrade the cooling section could be covered by very weak helical undulators), due to recombination lifetime being much longer than beam lifetime associated with other effects.

Magnetic shielding

To keep transverse angles of electron beam at an acceptable level an integral of residual transverse magnetic field in the space used for cooling should be kept to 1 Gauss·cm (at γ=4, for example). Shielding of residual magnetic field to such a level (about 5 mGauss) may be provided by two or three concentric cylindrical layers of high initial permeability alloy. The resulting total attenuation for DC fields will be more than a factor of 1000, for a safety margin.

Another approach of active control with Helmholtz coils is also being considered.

Correction solenoids

Some space is taken up by six very short weak (200 Gauss) solenoids (to control angular spread due to the space charge), steering dipoles and beam position monitors used to keep the electron beam and ion beam in close relative alignment.

Since electron beam does not have any magnetization space used by focusing solenoids will be lost from the cooling process. Presently, design of 5 inch ID solenoids is being optimized to maximize the space between solenoids which satisfy requirement on the integral of transverse magnetic field (1 Gauss·cm, at γ=4, for example). To allow for about 12 meters of effective cooling, full length of cooling section including solenoids is presently 14 m.

8 TRANSPORT MAGNETS

The length of electron beam transport line from the SRF accelerator to the cooling section is 11 m and includes 4 solenoids for matching beam optics functions (Fig. 11). Then there is a dog-leg merger to the RHIC blue ring which consists of two 45° chevron type dipole magnets with two solenoids in between (triplet of quadupoles can be considered as well).

First two meters of cooling section is used for matching of electron beam (telescope based on two solenoids 2 meters apart) with required optics for the cooler. This is followed by 14 meters (includes short 10cm focusing solenoids every 2 m) of space used for cooling. After 14 meters of cooling section there is a turn-around electron beam transport (dog bone in Fig. 20) which

consists of two telescopes for matching with two solenoids each and eight 45° chevron type dipole magnets.

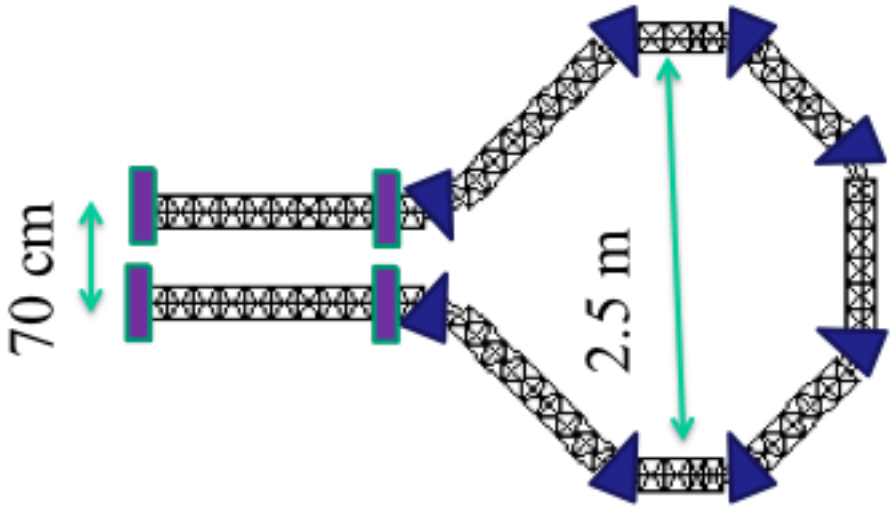

Figure 20. Dog bone turn around transport line from blue ring cooling section to yellow ring cooling section.

Total numbers of magnet elements:

Number=16: 45° dipoles, Gap 13 cm, maximum field 500 Gauss; R=38.2 cm, Lm=30 cm

Number=12: Solenoids ID 13 cm, maximum field 1.3 kGauss, Lmag=10cm

Number=6: Trim quadrupoles ID 13 cm L=10 cm maximum gradient TBD (might be needed to be installed for better matching)

Number=6: Cooling section solenoids ID 13cm, maximum field 0.2 kGauss, Lmag=10cm

An important feature of beam transport is that magnets should provide stable operation in full range of electron beam energies: 0.9-5 MeV.

9 VACUUM SYSTEM

The vacuum system close to SRF cavities requires particulate-free vacuum system. The rest of the transport beam line should have 10^{-9} Torr vacuum. The vacuum system of beam lines should have two automatic valves at the ends of the doglegs to shut them from RHIC vacuum in case of an unlikely vacuum accident.

The transport lines should have the pipe size of 3'' ID. Presently, the cooling sections in RHIC have vacuum chamber with 5" ID. Reduction of aperture for the cooling section to 3'' ID will be considered in detail.

The project will use the cryogenic system developed for the CeC PoP experiment in the same location.

10 BEAM DIAGNOSTICS

Preliminary set of the diagnostics is listed below:
1. Two in-flange Bergoz integrating current transformers (ICT) with beam charge monitors.
2. Fluorescent screens will be used for beam profile and position monitoring.
3. Low energy emittance measurements system will utilize pepper-pot set-up.
4. Two in-flange DC current transformers.
5. Beam Position Monitors.
6. RHIC wall current monitor will be used to measure profiles of ion bunches.
7. Spectrum analyzer to monitor ion beam spectrum evolution.
8. Beam loss monitors to observe losses of charged particle (both ions and electrons).

Beam Position Monitors

The ion beam position will be monitored with existing RHIC pick-up electrodes (striplines). The electron beam position will be monitored with button type pick-up electrodes.

BPMs will be used for overlapping of the ion and electron beams. They will also be used for beam based alignment of the solenoids in order to reach required electron beam trajectory.

Each cooling section will have four BPMs – two in the beginning and two at the end for redundancy. The BPMs can be used for the loss monitoring of the electron beam and provide interlock signal on the beam deviation from the predetermined limits.

Current Monitoring

The electron beam current will be monitored with two DCCTs one placed after the accelerator and one before the beam dump. Two measurement heads are needed to monitor beam losses and will provide interlock signal if losses exceed the defined level. At low current (low repetition rate) the noise in the DCCT makes them not usable and integrating current transformers will be utilized.

Transverse Emittance in both planes

An emittance station will be installed just downstream of the SRF accelerating cavity to measure the beam parameters. Tungsten masks with slits will be plunged in upstream of a YAG:Ce screen profile monitor to measure transverse emittance.

Energy Spread and Bunch Length

The flag will be placed in the merger section of the ion and electron beams in the location with non-zero dispersion. Knowledge of the horizontal emittance will allow us to calculate the beam energy spread. By accelerating off-crest in the accelerating cavity we will get information about the bunch length from the measured growth of the beam energy spread.

Electron & Ion Beam Synchronization

Electron bunches will be synchronized with ion bunches. Laser will produce pulses with 100 MHz frequency and required bunch pattern.

11 REFERENCES

[1] A. Fedotov, I. Ben-Zvi, X. Chang, D. Kayran, T. Satogata, Proc. of COOL'07 workshop (Bad Kreuznach, Germany), p. 243 (2007).

[2] A. Fedotov, I. Ben-Zvi, X. Chang, D. Kayran, V. Litvinenko, E. Pozdeyev and T. Satogata, BNL Collider-Accelerator Department Tech Note: C-A/AP/307 (April 2008).

[3] A. Fedotov, I. Ben-Zvi, X. Chang, D. Kayran, V. Litvinenko, E. Pozdeyev, T. Satogata, Proc. of HB2008 workshop (Nashville, TN), p. 75, WGA10 (2008).

[4] A. Fedotov, M. Blaskiewicz, W. Fischer, T. Satogata, S. Tepikian, Proc. of HB2010 workshop (Morschah, Switzerland), p. 634, THO1C03 (2010).

[5] A. Fedotov, M. Bai, M. Blaskiewicz, W. Fischer, D. Kayran, C. Montag, S. Tepikian, G. Wang and T. Satogata, Proc. of PAC'11 conference (New York, NY), p. 2285, THP081 (2011).

[6] C. Montag, BNL Collider-Accelerator Department Tech Note: C-A/AP/421 (January 2011).

[7] C. Montag et al., BNL C-AD Tech Note: C-A/AP/435 (October 2011).

[8] C. Montag et al., Dynamic aperture limitation for 2.5 GeV operation (2013).

[9] A. Fedotov and M. Blaskiewicz, "Potential for luminosity improvement for low-energy RHIC operation with long bunches", BNL C-AD Tech Note: C-A/AP/449 (February 2012).

[10] V. Litvinenko, "Choosing RF system for low energy RHIC operation", BNL Collider-Accelerator Department Tech Note: C-A/AP/476 (December 2012).

[11] A. Fedotov, "Projections of potential luminosity improvement for low-energy RHIC operation with electron cooling", BNL C-AD Tech Note: C-A/AP/481 (April 2013).

[12] A. Fedotov, "IBS below transition energy and various RF systems", BNL Collider-Accelerator Department Tech Note: C-A/AP/477 (February 2013).

[13] D. Dowell, et al., "First operation of a photocathode radio frequency gun injector at high duty factor," *Appl. Phys. Lett.* **63**, 2035 (1993).

[14] B. Dunham, et al., "Record high-average current from a high-brightness photoinjector," *Appl. Phys. Lett.* **102**, 034105 (2013).

[15] D. H. Dowell, "Cathode R&D for future light sources," *Nucl. Instr. and Meth. in Phys. Res. A* **622** (2010) 685-697.

[16] A. Arnold and J. Teichert, "Overview on superconducting photoinjectors," *Phys. Rev. ST Accel. Beams* **14** (2011) 024801.

[17] R. Mammei, et al., "Charge lifetime measurements at high average current using a K_2CsSb photocathode inside a dc high voltage photogun," *Phys. Rev. ST Acc Beams* **16** (2011) 033401.

[18] S. Belomestnykh, "Survey of SRF guns," *Proc. SRF2011* (Chicago, IL, USA, 2011), p. 23-26.

[19] S. Belomestnykh, et al., "Superconducting 112 MHz QWR electron gun," *Proc. SRF2011* (Chicago, IL, USA, 2011), pp. 223-225.

[20] T. Xin, et al., "Design of the fundamental power coupler and photocathode inserts for the 112 MHz superconducting electron gun, *Proc. SRF2011* (Chicago, IL, USA, 2011), pp. 83–86.

[21] M. Kelly, et al., "Cold testing of superconducting 72 MHz quarter-wave cavities for ATLAS," *Proc. LINAC2012* (Tel-Aviv, Israel, 2012), pp. 348-350.

[22] Z. Conway, et al., "Reduced-beta cavities for high-intensity compact accelerators," *Proc. LINAC2012* (Tel-Aviv, Israel, 2012), pp. 458-460.

[23] B. Mustapha (ANL), private communications.